Cell Calcium

TNF-α and IL-1β increase Ca²⁺ leak from the sarcoplasmic reticulum and susceptibility to arrhythmia in rat ventricular myocytes

David J. Duncan [a], Zhaokang Yang [a], Philip M. Hopkins [b], Derek S. Steele [a], Simon M. Harrison [a],*

[a] Multidisciplinary Cardiovascular Research Centre, Institute of Membrane and Systems Biology, University of Leeds, Leeds, LS2 9JT, UK
[b] Academic Unit of Anaesthesia, University of Leeds, Leeds, LS2 9JT, UK

ARTICLE INFO

ABSTRACT

Sepsis is associated with ventricular dysfunction and increased incidence of atrial and ventricular arrhythmia however the underlying pro-arrhythmic mechanisms are unknown. Serum levels of tumour necrosis factor-α (TNF-α) and interleukin-1β (IL-1β) are elevated during sepsis and affect Ca²⁺ regulation. We investigated whether pro-inflammatory cytokines disrupt cellular Ca²⁺ cycling leading to reduced contractility, but also increase the probability of pro-arrhythmic spontaneous Ca²⁺ release from the sarcoplasmic reticulum (SR). Isolated rat ventricular myocytes were exposed to TNF-α (0.05 ng ml⁻¹) and IL-1β (2 ng ml⁻¹) for 3 hr and then loaded with fura-2 or fluo-3 to record the intracellular Ca²⁺ concentration ([Ca²⁺]ᵢ). Cytokine treatment decreased the amplitude of the spatially averaged Ca²⁺ transient and the associated contraction, induced asynchronous Ca²⁺ release during electrical stimulation, increased the frequency of localized Ca²⁺ release events, decreased the SR Ca²⁺ content and increased the frequency of spontaneous Ca²⁺ waves at any given cytoplasmic Ca²⁺. These data suggest that TNF-α and IL-1β increase the SR Ca²⁺ leak from the SR, which contributes to the depressed Ca²⁺ transient and contractility. Increased susceptibility to spontaneous SR Ca²⁺ release may contribute to arrhythmias in sepsis as the resulting Ca²⁺ extrusion via NCX is electrogenic, leading to cell depolarisation.

© 2010 Elsevier Ltd. Open access under CC BY-NC-ND license.

1. Introduction

Sepsis is associated with ventricular dysfunction (e.g. [1]) and increased incidence of atrial and ventricular arrhythmia (e.g. [2]) which contribute to poor prognosis for patients [3]. Pro-inflammatory cytokines, such as tumour necrosis factor-α (TNF-α) and interleukin-1β (IL-1β), have been implicated in ventricular dysfunction associated with a variety of pathological conditions, including reperfusion injury and sepsis [4–7]. Furthermore, TNF-α and IL-1β appear to act synergistically to depress ventricular contractility at much lower concentrations than is required by each cytokine alone [6].

The mechanisms proposed to explain the direct inhibitory effects of these cytokines in ventricular tissue typically involve altered Ca²⁺ regulation, although a number of disparate pathways have been suggested, e.g. (i) altered sphingomyelin metabolism leading to an increase in sphingosine concentration, which acts to decrease the open probability of SR Ca²⁺ channels (ryanodine receptors, RyR2; [8]), or (ii) elevation of nitric oxide (NO) [9–12], followed by S-nitrosylation of RyR2 [13], leading to an increase in

RyR2 mediated Ca²⁺ leak and depletion of SR Ca²⁺ [14]. This latter mechanism is consistent with data derived from a whole animal model of sepsis induced by caecal ligation and puncture (CLP) [15], where altered Ca²⁺ regulation was evidenced as an increase in Ca²⁺ leak from the SR (i.e. enhanced spark frequency). However, it is not clear whether the effects of cytokine-induced modulation of SR Ca²⁺ regulation also predispose ventricular cells to arrhythmia.

The aims of the present study were to establish (i) whether exposure of ventricular myocytes to low, clinically relevant concentrations of TNF-α and IL-1β could mimic the deleterious effects observed in CLP-induced sepsis [15] and (ii) whether cytokine treatment is associated with pro-arrhythmic spontaneous Ca²⁺ release from the SR which may contribute to the increased incidence of arrhythmia in sepsis.

2. Materials and methods

2.1. Cell isolation

The technique used to prepare rat ventricular myocytes has been described in detail elsewhere [16]. Briefly, healthy adult male Wistar rats weighing ~200–250 g were killed humanely using Schedule 1 techniques sanctioned by the United Kingdom government Home Office and the local ethical review committee. The heart was excised rapidly, the aorta cannulated and perfused via

the coronary arteries with a series of solutions based on a Ca^{2+} free 'isolation solution' (composition below). Initial perfusion was with isolation solution plus 750 μM $CaCl_2$ (equilibrated with 100% oxygen) to flush the coronary arteries of blood and once the heart was beating regularly, the perfusate was changed to isolation solution containing 100 μM EGTA for 4 min. The heart was then perfused for 6 min with isolation solution supplemented with 1.2 mg ml^{-1} collagenase (type 2, Worthington Biochemical Corp, Lakewood, NJ), 0.1 mg ml^{-1} protease (type XIV, Sigma, Poole, UK) and 80 μM $CaCl_2$. The ventricles were cut from the heart, chopped finely and agitated gently in enzyme solution (supplemented with 1% BSA) for 5 min intervals. Dissociated cells were harvested by filtration at the end of each 5 min interval and the remaining tissue subjected to further enzyme treatment. Dissociated cells were centrifuged at 30 × g for 60 s, resuspended in 750 μM $CaCl_2$ solution and stored at room temperature until use.

2.2. Solutions and cytokine treatment

The isolation solution was composed of the following (in mM): NaCl 130; KCl 5.4; $MgCl_2$ 1.4; NaH_2PO_4 0.4; HEPES 5; glucose 10; taurine 20; creatine 10; pH 7.1 (NaOH) at 30 °C. Normal Tyrode solution (NT) contained (in mM): NaCl 140; KCl 5.4; $MgCl_2$ 1.2; NaH_2PO_4 0.4; HEPES 5; glucose 10; $CaCl_2$ 1; pH 7.4 (NaOH) at 30 °C. TNF-α (Sigma, Poole, UK) was prepared in 10% BSA and diluted to 0.05 ng ml^{-1} from a stock solution of 2.5 μg ml^{-1} and IL-1β (2 ng ml^{-1}) was diluted from a stock solution of 1 μg ml^{-1} (Sigma) in NT solution.

Cells were incubated in either NT solution (control cells) or NT supplemented with TNF-α (0.05 ng ml^{-1}) and IL-1β (2 ng ml^{-1}) for 180 min as described previously [17,18]. 10 min before the end of the incubation, cells were loaded with fura-2 [17] or fluo-3 [19]. Cells were centrifuged as before, the supernatant removed and the pellet resuspended in incubation solution. Fura-2 and fluo-3 loaded cells were left for ~15 min before use to allow for de-esterification of the dye to take place.

2.3. Cell length and conventional Ca^{2+} transient measurement

Cells were transferred to a tissue chamber (volume <200 μl) attached to the stage of an inverted microscope (Nikon; Tokyo; Japan) and allowed to settle for several minutes. Control cells were superfused continuously with NT solution whereas treated cells were superfused with NT supplemented with TNF-α (0.05 ng ml^{-1}) and IL-1β (2 ng ml^{-1}). Cells were stimulated at a frequency of 1 or 3 Hz (stimulus duration 2 ms) via two platinum electrodes situated in the side of the tissue chamber. Cell length was assessed optically (IonOptix Corporation, Milton, MA) and digitized at 200 Hz. The whole cell cytosolic Ca^{2+} transient was recorded in fura-2 loaded cells excited alternately at 340 and 380 nm using a monochromator system (Cairn, Kent, UK) and the emitted fluorescence was detected at 510 ± 40 nm. The fluorescence ratio (Fr) was digitised at 1 kHz using IonOptix software. Although most experiments were carried out at 30 °C, qualitatively similar effects of TNF-α and IL-1β were obtained at 22 °C (not shown).

2.4. Confocal imaging of intact and skinned myocytes

Confocal imaging was performed using a laser-scanning unit (BioRad Microradiance 2000, Welwyn Garden City, UK) attached to a Nikon Diaphot inverted microscope (Nikon; Tokyo; Japan). The X–Y resolution of the system was 0.45 μm, as measured from the point-spread function of fluorescent microspheres (diameter 0.175 μm). The aperture size was set to the size of the Airy disc to optimize z-axis resolution. Fluo-3 was excited with the 488-nm line

of an argon ion laser and fluorescence measured at >515 nm. Line-scan images were acquired at 6 or 2 ms intervals along the length of the cell. To reduce possible laser damage, the position of the line was changed after two to three scan sequences. Data were analyzed using ImageJ (NIH, USA, http://rsbweb.nih.gov/ij/) and Image Pro-Plus version 5.1 (Media Cybernetics Europe, Marlow, Buckinghamshire, UK). The automated detection of Ca^{2+} sparks and the measurement of temporal and spatial properties was carried out using the "Sparkmaster" plugin for ImageJ [20]. Spark width and duration was measured at full width half maximum (FWHM) and full duration half maximum (FDHM), respectively.

2.5. Solutions for confocal Ca^{2+} measurement in intact and permeabilized myocytes

Intact myocytes were superfused with NT solution at room temperature. Cells were permeabilized by exposure to saponin (10 μg ml^{-1}) for 6 min in weakly Ca^{2+}-buffered solutions approximating to the intracellular milieu, before centrifugation and re-suspension. The mock intracellular solution contained (in mM): KCl, 100; HEPES, 25; EGTA, 0.05–0.36; phosphocreatine 10; ATP, 5 and fluo-3, 0.001, pH 7.0, 22 °C. $MgCl_2$ was added (from 1 M stock solution) to produce a free concentration of 1.0 mM. The free [Ca^{2+}] was adjusted by addition of $CaCl_2$.

2.6. Statistical analysis

Data are presented as mean ± s.e.m. and unless otherwise stated, each data set was derived from cells isolated from a minimum of five animals. Statistical comparisons of multiple control and treated groups were performed using paired or unpaired t-test or ANOVA with post hoc tests (Holme Sidak) as appropriate. If data failed a normality test (Kolmogorov–Smirnov) an appropriate non-parametric test was carried out. Significant results, unless stated otherwise have a P value <0.05.

3. Results

The contraction amplitude (expressed as percentage of resting cell length) and Ca^{2+} transient amplitude were both significantly ($P < 0.05$) reduced (to 54% and 65% of control, respectively) in cells treated for 180 min with TNF-α and IL-1β (Fig. 1A–C). No significant difference was observed in the time for half decay of either contraction ($P = 0.326$) or the Ca^{2+} transient ($P = 0.583$) between control ($n = 64$) and treated cells ($n = 58$).

As described above, TNF-α and IL-1β have been reported to act synergistically to reduce contractility in ventricular tissue. This is illustrated in Fig. 1D, where cells were incubated in either TNF-α (0.05 ng ml^{-1}) or IL-1β (2 ng ml^{-1}) alone for 180 min. Neither TNF-α nor IL-1β had a significant effect on contraction amplitude ($P = 0.758$ and 0.789, respectively), Ca^{2+} transient amplitude ($P = 0.317$ and 0.313) or the time course of either contraction ($P = 0.747$ and 0.359) or the Ca^{2+} transient ($P = 0.918$ and 0.275), when compared with control cells incubated in NT for the same time period.

To assess the ability of control and treated cells to respond to a positive inotropic intervention, the stimulation rate was increased from 1 to 3 Hz. This significantly increased cell contraction, Ca^{2+} transient magnitude, diastolic [Ca^{2+}] and the SR Ca^{2+} content (estimated from the peak of a caffeine-induced Ca^{2+} transient) in both control and treated cells. However, these parameters (except diastolic [Ca^{2+}]) remained significantly depressed in cytokine-treated compared to control cells at 3 Hz (Fig. 2A–D). Frequency-dependent acceleration of relaxation and Ca^{2+} transient decay occurred under both control and treated conditions, but no significant differences between control and treated cells were observed (Fig. 2E and F).
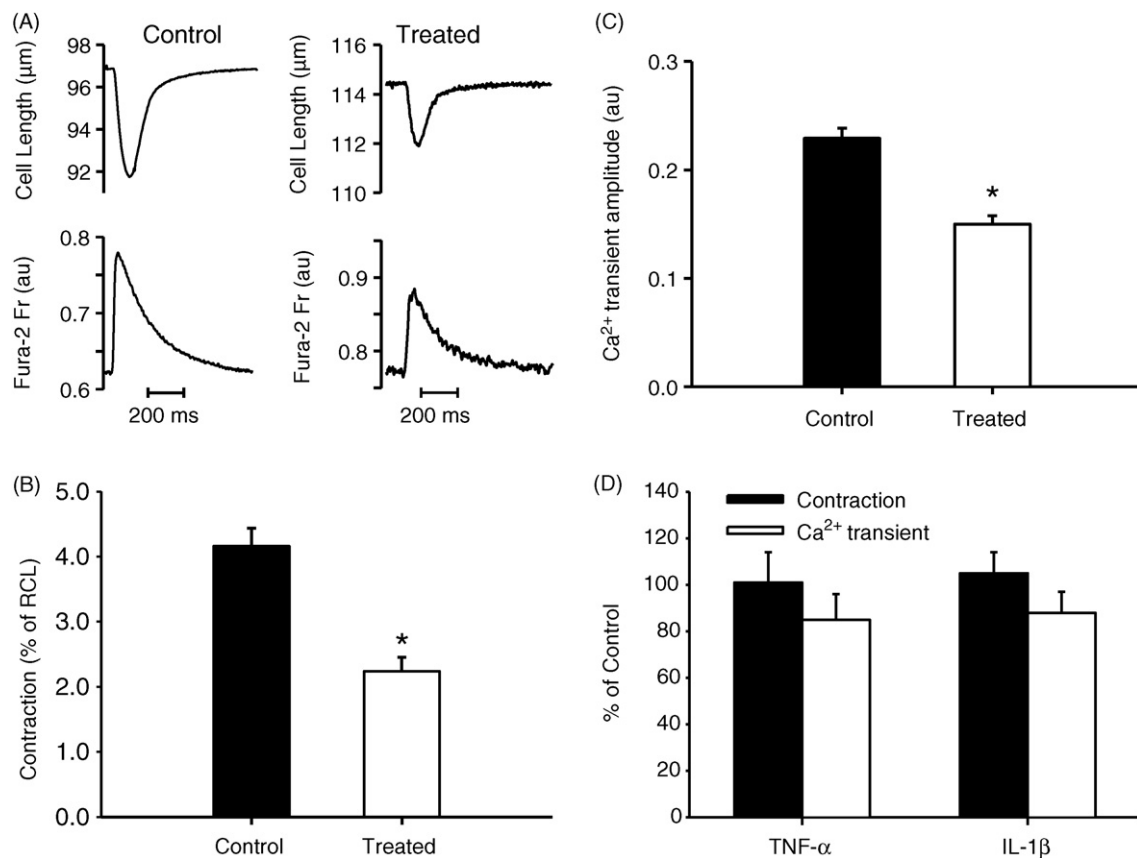
Fig. 1. (A) Fast time base records of cell length and Ca²⁺ transients from cells following 180 min incubation in either normal Tyrode's solution (NT) or NT supplemented with 0.05 ng ml⁻¹ TNF-α and 2 ng ml⁻¹ IL-1β. Mean data for control (n = 80) and treated, cells (n = 82) on contraction amplitude (B) and magnitude of the cytosolic Ca²⁺ transient (C). (D) The effects of 180 min exposure to TNF-α (0.05 ng ml⁻¹, n = 13) and IL-1β (2 ng ml⁻¹, n = 14) alone on contraction and the Ca²⁺ transient amplitude. *P < 0.05.

Fractional release of Ca²⁺ from the SR was determined by expressing the Ca²⁺ transient amplitude as a percentage of the SR Ca²⁺ content at 1 and 3 Hz stimulation. In control cells, fractional release was 63 ± 4% and 62 ± 4% at 1 and 3 Hz (P = 0.698), and in treated cells was 54 ± 4% and 50 ± 4% at 1 and 3 Hz (P = 0.078), respectively. At 1 Hz there was no significant difference between the fractional release of control and treated cells (P = 0.151) whereas at 3 Hz fractional release of treated cells was significantly reduced compared to control cells (P = 0.044).

Fig. 3 shows representative confocal line-scan images of control and treated cells with 3D surface plots of individual sparks for each condition; the latter demonstrating cytokine-induced changes in spark duration and width, which would increase spark mass (the volume integral of $\Delta F/F$) [21,22]. Cytokine treatment led to an increase in spark frequency (Fig. 3A and B) from 0.6 ± 0.1 s⁻¹ in quiescent control cells to 2.5 ± 0.1 s⁻¹ after 180 min of TNF-α and IL-1β treatment. Spark amplitude was not significantly affected by cytokine treatment (P > 0.05, t-test, Fig. 3B), however, spark duration and width were both increased significantly (by 18 ± 3% and 15 ± 4%, respectively, P < 0.05, n = 19, Fig. 3B) compared to control.

To assess whether cytokine-induced changes in spark characteristics were still evident following cell permeabilization, myocytes were first incubated for 180 min as above and then transferred to a mock intracellular solution (see Section 2) containing 10 μg ml⁻¹ saponin. Following cell permeabilization, the properties of Ca²⁺ sparks in cells treated with TNF-α and IL-1β were not significantly different from those measured in control cells (P > 0.05, n = 6). This remained the case whether or not TNF-α and IL-1β was present after permeabilization. This finding suggests that the effects of TNF-α and IL-1β are mediated by a diffusible second messenger, which cannot accumulate in permeabilized cells, rather than sustained changes to RyR2 gating.

Fig. 4A illustrates global Ca²⁺ release in electrically stimulated control (left panel) and treated (right panel) cells, assessed from line-scan images. In control cells (Fig. 4 left panels), electrical stimulation led to a synchronous rise of Ca²⁺ throughout the cell (Fig. 4A) which can be quantified by the fluorescent intensity profile labelled (i) at the time of stimulation (Fig. 4A and B). Fig. 4C illustrates that the temporal characteristics of the Ca²⁺ transient are similar through out the cell (see time course of Ca²⁺ transients generated by line profiles (ii) and (iii); Fig. 4A and C). However, in some treated cells (Fig. 4 right hand panels) the time course of Ca²⁺ release showed spatial heterogeneity (see line profile (iv)) at the time of stimulation in Fig. 4B and altered configuration of Ca²⁺ transients generated from different regions of the cell (line profiles (v) and (vi) in Fig. 4A and C). In control conditions, 5 out of 42 cells exhibited some evidence of asynchronous release whereas in cytokine-treated cells, this was increased significantly to 15 out of 49 cells (P < 0.01, Chi-squared test).

Fig. 5A shows an example of chaotic "diastolic" Ca²⁺ release in a field stimulated myocyte following cytokine treatment. A number of different forms of spontaneous Ca²⁺ release are apparent including Ca²⁺ sparks, larger non-propagating Ca²⁺ release events and fully propagating Ca²⁺ waves, which in this case originated at one end of the cell. Fig. 5B (upper panel) shows line-scan (left) and surface plot (right) images from a control cell following field stimulation. Control cells typically exhibited a quiescent period immediately after each stimulation, when Ca²⁺ sparks were not apparent or occurred at very low frequency. Also shown is a line-
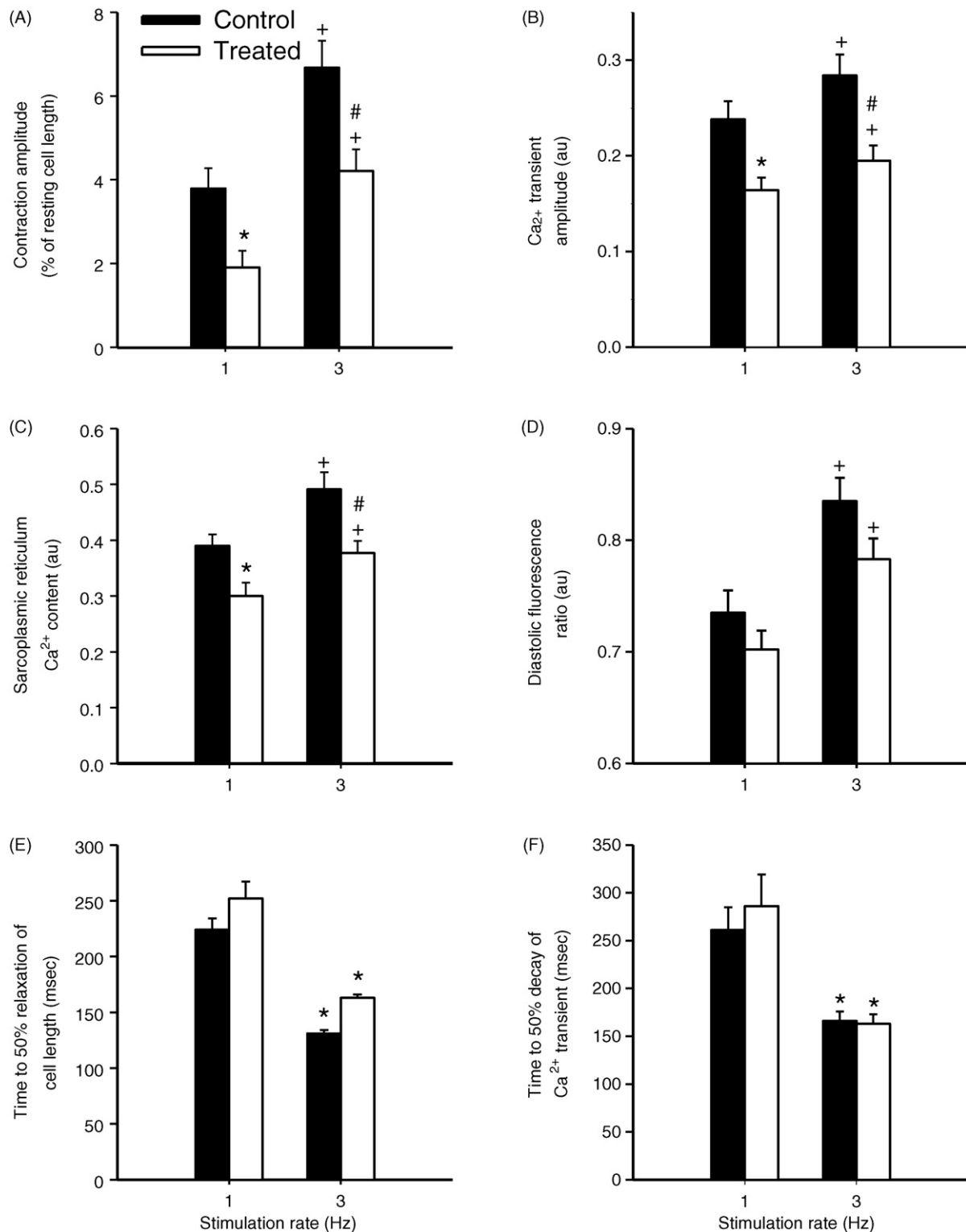
Fig. 2. Mean data describing contraction amplitude (A), Ca^{2+} transient amplitude (B), SR Ca^{2+} content (C) and diastolic fluorescence ratio (D) of control ($n=27$) and treated ($n=24$) cells during 1 and 3 Hz stimulation. At 1 Hz, cytokine treatment significantly decreased cell contraction, the Ca^{2+} transient and SR Ca^{2+} content (*$P<0.05$ vs 1 Hz control, t-test). At 3 Hz all parameters were significantly increased (+$P<0.001$, paired t-test vs 1 Hz) in both control and treated cells however cell contraction, the Ca^{2+} transient and SR Ca^{2+} content remained significantly depressed compared to control (#$P<0.05$ vs 3 Hz control, t-test). Rate-dependent decreases in the time for half decay of contraction (**E**) and the Ca^{2+} transient (**F**) were observed at 3 Hz in both control and treated cells (*$P<0.05$, paired t-test vs 1 Hz) but this was unaffected by cytokine treatment.

scan image and corresponding surface plot from a cell treated with TNF-α and IL-1β under similar conditions (lower panel). Treated cells typically exhibited Ca^{2+} sparks during and immediately after each stimulated response. The non-uniform rising phase

of the stimulated Ca^{2+} transient is also apparent in this example. Fig. 5C shows cumulative data from experiments in which control (left) or cytokine-treated (right) cells were stimulated at 6 s intervals and the frequency of diastolic Ca^{2+} sparks measured as
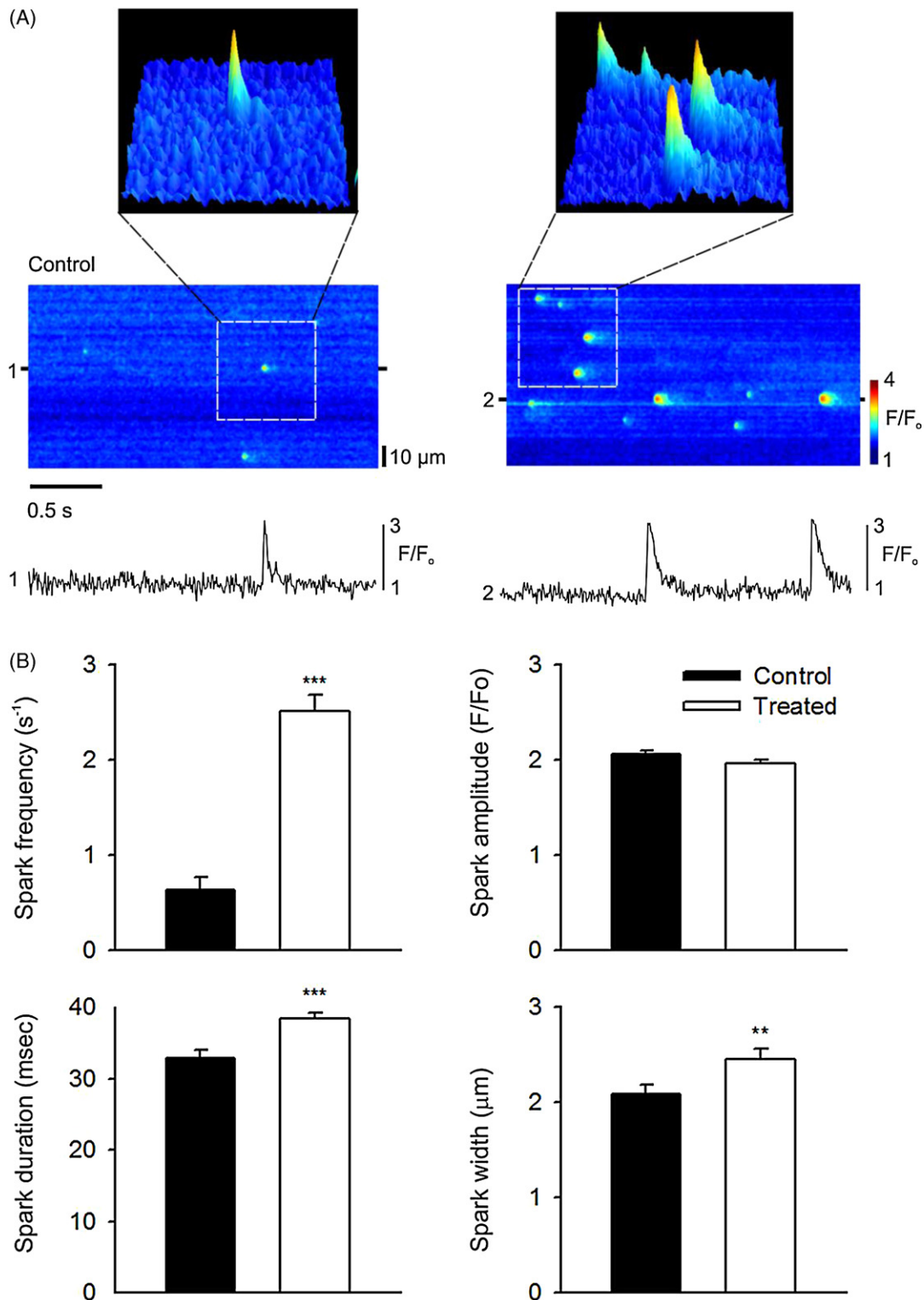
Fig. 3. (A) Typical line-scan images of Ca^{2+} sparks from myocytes under control conditions (left) or following incubation with TNF-α and IL-1β (right). Surface plots are from the regions of each line-scan indicated. Selected line profiles are also shown below each image (1,2). These were produced by averaging 3 pixels centred on the peak of the Ca^{2+} sparks. (B) Mean data describing spark frequency (s^{-1}) per 100 μm, amplitude (F/F_0), duration (FDHM) and width (FWHD) in control and treated cells ($n = 19$ per group). ***$P < 0.001$ vs control, **$P < 0.05$ vs control, t-test.

a function of time. In control cells the quiescent period immediately after each stimulated response was followed by a progressive increase in spark frequency over the subsequent 5 s. However, in treated cells, the mean spark frequency was higher and there was no apparent relationship between spark frequency and time after stimulation.

Fig. 6A illustrates changes in the frequency of spontaneous Ca^{2+} waves in an unstimulated cell at different extracellular Ca^{2+}. Elevation of Ca^{2+} from 1 to 3 mM led to a significant increase in wave frequency in both control and treated cells. However, at any given extracellular Ca^{2+} concentration, wave frequency was significantly higher in cytokine-treated cells.
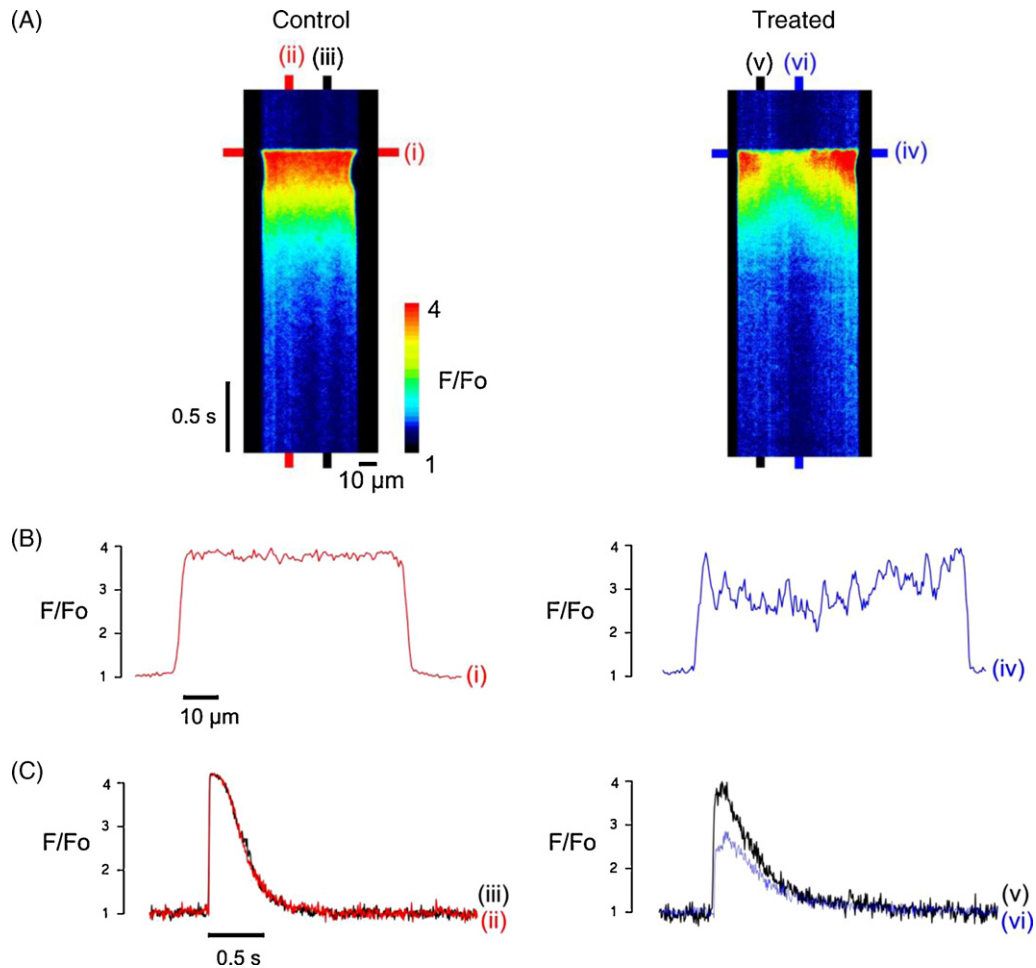
Fig. 4. (A) Typical line-scan images obtained during field stimulation from control (left) and treated (right) cells displaying synchronous or asynchronous Ca^{2+} release, respectively. (B) Line profiles positioned transversely across the image (i and iv), at the point of stimulation. (C) Superimposed longitudinal line profiles indicating the time course and amplitude of the Ca^{2+} transients at the points indicated (ii and iii for control (left) and v and vi for treated cells (right)). All line profiles were obtained by averaging over 3 pixels.

4. Discussion

Incubation of isolated ventricular myocytes in TNF-α and IL-1β for 180 min was associated with a decrease in cell contractility, the amplitude of the spatially averaged Ca^{2+} transient and the SR Ca^{2+} content, while Ca^{2+} spark frequency increased (Figs. 1–3). These data are similar to results obtained from myocytes isolated from rat hearts, 48 h after induction of sepsis in vivo via CLP [15]. Importantly, this shows that although CLP would be expected to lead to expression of a variety of both pro- and anti-inflammatory cytokines, the changes observed in contractility and SR Ca^{2+} release can be mimicked by the combined actions of TNF-α and IL-1β alone.

4.1. Effects TNF-α and IL-1β on Ca^{2+} sparks

The decrease in contractility following cytokine treatment likely reflects the smaller amplitude of the whole cell Ca^{2+} transient (Fig. 1), which is consistent with the reduced SR Ca^{2+} content (Fig. 2). The lower SR Ca^{2+} content can in turn be explained by the increase in SR Ca^{2+} leak, manifested as a sustained increase in Ca^{2+} spark frequency (Fig. 3). However, although this interpretation appears likely in the context of the present study, modulation of RyR2 function alone does not typically induce sustained changes in SR Ca^{2+} release.

In paced ventricular myocytes, a moderate increase in the open probability of RyR2 (e.g. with sub-millimolar caffeine) induces only a transient increase in the whole cell Ca^{2+} transient [23]. This intrinsic "autoregulation" is also apparent with localised Ca^{2+} release events in quiescent cells (and with a variety of RyR2 modulators), where Ca^{2+} spark frequency increases transiently before returning to the control level [24]. In general, therefore, interventions that increase the open probability of RyR2 have no sustained effect. Indeed, sustained increases in Ca^{2+} spark frequency are generally associated with factors that *increase* the SR Ca^{2+} content, reflecting an increase in the influence of luminal Ca^{2+} on RyR2 [24].

Against this background, the sustained increase in Ca^{2+} spark frequency associated with TNF-α and IL-1β treatment, combined with a decrease in SR Ca^{2+} content, was unexpected. However, one possible explanation for this apparent discrepancy is that exposure to TNF-α and IL-1β might alter regulation of RyR2 by SR luminal Ca^{2+}, e.g. following cytokine treatment, the sustained increase in Ca^{2+} spark frequency might reflect an abnormally large influence of SR luminal Ca^{2+} on RyR2, despite the lower SR Ca^{2+} content. Consistent with this interpretation, spark frequency was little affected by SR Ca^{2+} depletion initiated by field stimulation in cytokine treated cells (Fig. 5B and C). This contrasts with the typical response of control myocytes, which exhibit a quiescent period immediately following the Ca^{2+} transient, during which sparks are less frequent, followed by a gradual increase in spark frequency. Indeed, in treated cells, Ca^{2+} sparks were often apparent both during the descending phase and immediately after triggered Ca^{2+} transients.
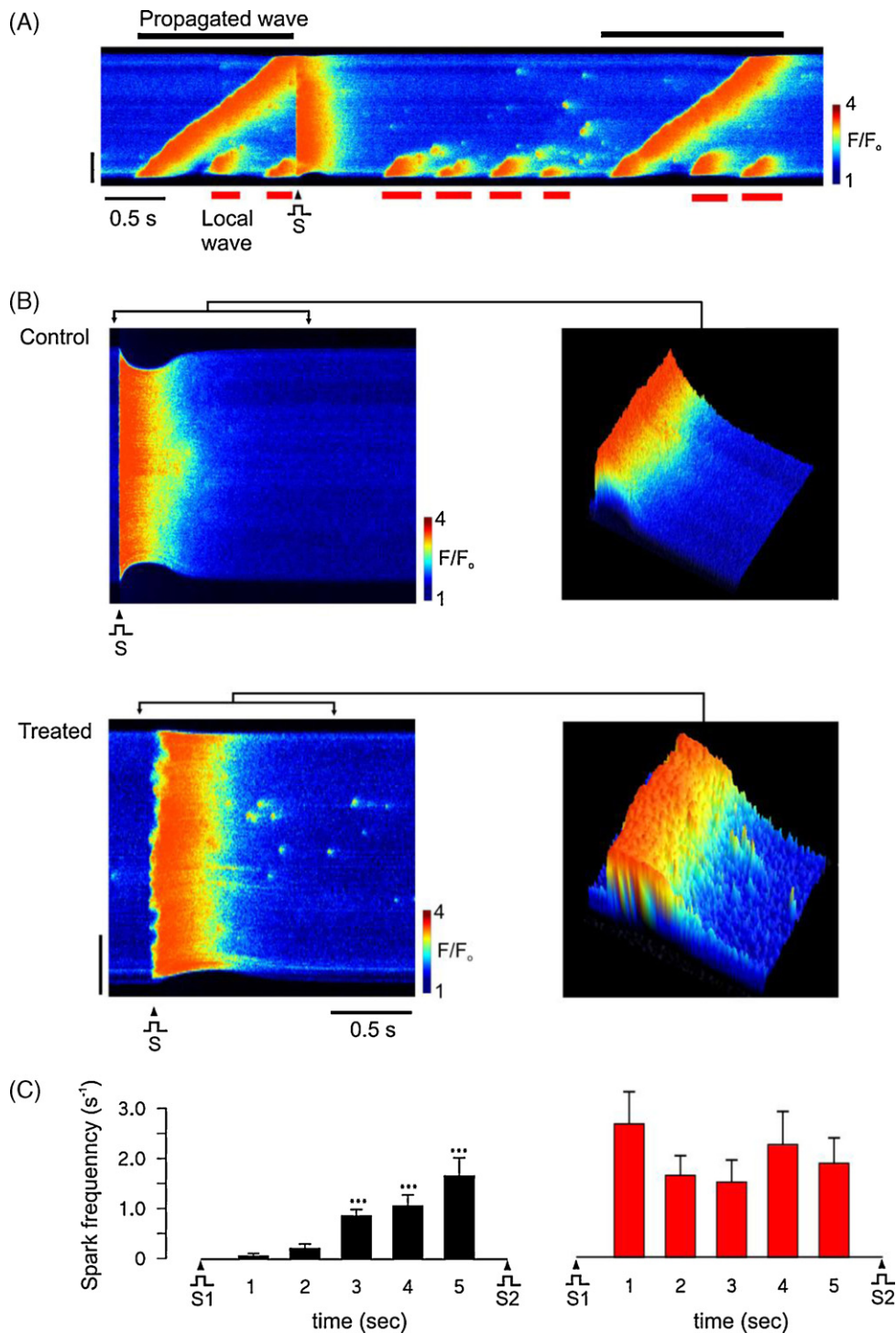
Fig. 5. (A) Representative data showing field stimulated Ca^{2+} transients interspersed with local Ca^{2+} release (red bars) and propagated waves (black bars) in a cytokine-treated cell. (B) Line-scan image and surface plot from a control cell following field stimulation (upper panel). Control cells typically exhibit a quiescent period immediately after each stimulation, when Ca^{2+} sparks were not apparent or occurred at very low frequency. Also shown is a line-scan image and corresponding surface plot from a cell treated with TNF-α and IL-1β under similar conditions (lower panel). Treated cells typically exhibited Ca^{2+} sparks during and immediately after each stimulated response. (C) Cumulative data showing changes in spontaneous Ca^{2+} spark frequency (s^{-1}) per 100 μm, from control (left) and treated (right) cells stimulated at 6 s intervals. In control cells ($n = 20$) spark frequency progressively increased from a very low level immediately after the initial stimulation. In treated cells ($n = 28$) there was no clear temporal relationship between the time and spark frequency. ***Value significantly different from that at 1 s ($P < 0.001$). Vertical bar indicates 25 μm. 'S' indicates field stimulation.

4.2. Asynchronous Ca^{2+} release following exposure to TNF-α and IL-1β

The frequency of Ca^{2+} sparks increases as a function of the SR Ca^{2+} content until a point is reached when propagation occurs between neighbouring release sites [25]. The resulting wave of Ca^{2+}-induced Ca^{2+} release (CICR) induces global SR Ca^{2+} depletion, thereby dictating the maximum SR Ca^{2+} content. Recent work has shown that the transition to Ca^{2+} wave propagation is predominantly due to the sensitizing influence of SR luminal Ca^{2+} on RyR2
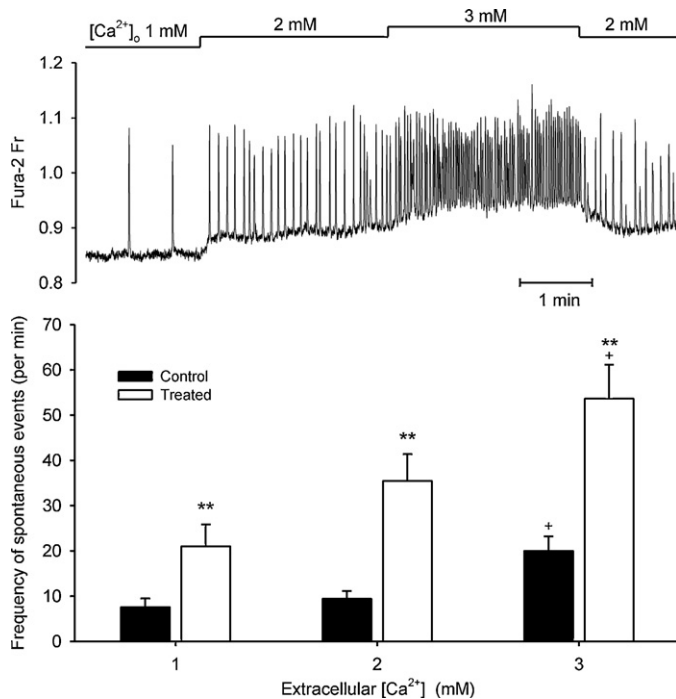
Fig. 6. (A) Representative record of spontaneous Ca^{2+} waves recorded in a control unstimulated cell at extracellular $[Ca^{2+}]$ of 1, 2 and 3 mM. (B) Mean data describing the frequency of spontaneous Ca^{2+} waves in control ($n = 7$–9) and treated ($n = 8$) cells. Frequency was increased significantly ($**P < 0.01$) in treated cells compared to control cells at any given extracellular $[Ca^{2+}]$ and in both control and treated cells between 1 and 3 mM extracellular Ca^{2+} ($^{+}P < 0.01$).

[26]. Indeed, both Ca^{2+} sparks and waves can be considered to be events driven by the activity of SERCA and consequent effects mediated via SR luminal Ca^{2+}. This mechanism is clearly distinct from triggered CICR, where Ca^{2+} influx and subsequent binding to regulatory sites located on the large cytosolic domain underlies RyR2 activation.

In the present study, TNF-α and IL-1β had apparently different effects on spontaneous and triggered forms of SR Ca^{2+} release. Triggered Ca^{2+} release was significantly reduced in amplitude (Fig. 1) and this was accompanied by local release failure and asynchrony in the rising phase of the Ca^{2+} transient (Fig. 4). This contrasts with the facilitation of both spontaneous Ca^{2+} sparks and waves, despite the decrease in SR Ca^{2+} content.

One possible explanation for this difference is that a primary effect of TNF-α and IL-1β on spontaneous Ca^{2+} release might underlie the detrimental effects on triggered Ca^{2+} release. Specifically, RyR2 clusters involved in the generation of sparks just prior to electrical stimulation may be refractory to triggered CICR [27], decreasing both the synchrony and magnitude of global Ca^{2+} release (Fig. 4). In addition, triggered Ca^{2+} release exhibits a nonlinear dependence upon the SR Ca^{2+} content: a decrease in the average SR Ca^{2+} content to around 60% of the maximum content is sufficient to cause failure of triggered Ca^{2+} release in rat myocytes [28]. Therefore, the decrease in average SR Ca^{2+} content due to the increase in SR Ca^{2+} leak may also contribute to inhibition and asynchrony of the global Ca^{2+} transient.

4.3. Pro-arrhythmic changes in SR Ca^{2+} regulation

Sepsis is associated with increased incidence of both atrial and ventricular arrhythmia [2,29]. In the case of ventricular arrhythmias (ectopic beats, fibrillation or tachycardia), there is relatively little published data and the underlying causes are not clear. In the present study, exposure to TNF-α and IL-1β increased the fre-

quency of spontaneous Ca^{2+} waves at each extracellular $[Ca^{2+}]$ relative to control cells (Fig. 6). Spontaneous SR Ca^{2+} release is known to be pro-arrhythmic because the resulting Na/Ca exchange current is electrogenic, facilitating cell depolarisation, which can lead to delayed after depolarizations (DADs) [30]. DAD-induced triggered activity is established as an important class of arrhythmia linked to sudden cardiac death in circumstances where SR Ca^{2+} regulation is disturbed, e.g. ischemia, treatment with cardiac glycosides or with familial cardiomyopathies such as catecholaminergic polymorphic ventricular tachycardia (CPVT) [31]. In intact tissue, spontaneous depolarisations arising in single myocytes (or groups of associated cells) must overcome the electrotonic influence of neighbouring myocardial tissue before a propagated action potential can occur [32]. It seems likely that the higher frequency of spontaneous Ca^{2+} transients following treatment with TNF-α and IL-1β will increase the probability of this local threshold being exceeded, thereby predisposing to triggered arrhythmias.

In summary, this study illustrates that simultaneous exposure of ventricular myocytes to TNF-α and IL-1β reduces cell contractility, the magnitude of the Ca^{2+} transient and SR Ca^{2+} content, effectively mimicking effects seen in CLP-induced sepsis [15]. Enhanced spark frequency, propensity for spontaneous wave generation and subsequent triggered activity provides a pro-arrhythmic state which may contribute to the increased incidence of arrhythmia observed clinically in patients with sepsis.

References

[1] A. Kumar, C. Haery, J.E. Parrillo, Myocardial dysfunction in septic shock, Crit. Care Clin. 16 (2000) 251–287.
[2] A. Schwartz, G. Gurman, G. Cohen, H. Gilutz, S. Brill, M. Schily, B. Gurevitch, Y. Shoenfeld, Association between hypophosphatemia and cardiac arrhythmias in the early stages of sepsis, Eur. J. Intern. Med. 13 (2002) 434.
[3] A. Rudiger, M. Singer, Mechanisms of sepsis-induced cardiac dysfunction, Crit. Care Med. 35 (2007) 1599–1608.
[4] G. Baumgarten, P. Knuefermann, D.L. Mann, Cytokines as emerging targets in the treatment of heart failure, Trends Cardiovasc. Med. 10 (2000) 216–223.
[5] L.C. Casey, R.A. Balk, R.C. Bone, Plasma cytokine and endotoxin levels correlate with survival in patients with the sepsis syndrome, Ann. Intern. Med. 119 (1993) 771–778.
[6] A. Kumar, V. Thota, L. Dee, J. Olson, E. Uretz, J.E. Parrillo, Tumor necrosis factor alpha and interleukin 1β are responsible for in vitro myocardial cell depression induced by human septic shock serum, J. Exp. Med. 183 (1996) 949–958.
[7] C. Stamm, D.B. Cowan, I. Friehs, S. Noria, P.J. del Nido, F.X. McGowan Jr., Rapid endotoxin-induced alterations in myocardial calcium handling: obligatory role of cardiac TNF-α, Anesthesiology 95 (2001) 1396–1405.
[8] C.A. Dettbarn, R. Betto, G. Salviati, P. Palade, G.M. Jenkins, R.A. Sabbadini, Modulation of cardiac sarcoplasmic reticulum ryanodine receptor by sphingosine, J. Mol. Cell Cardiol. 26 (1994) 229–242.
[9] J.W. Horton, D. Maass, J. White, B. Sanders, Nitric oxide modulation of TNF-α-induced cardiac contractile dysfunction is concentration dependent, Am. J. Physiol. Heart Circ. Physiol. 278 (2000) H1955–H1965.
[10] X.W. Yu, Q. Chen, R.H. Kennedy, S.J. Liu, Inhibition of sarcoplasmic reticular function by chronic interleukin-6 exposure via iNOS in adult ventricular myocytes, J. Physiol. 566 (2005) 327–340.
[11] J.A. Mitchell, P. Gray, P.D. Anning, M. Woods, T.D. Warner, T.W. Evans, Effects of nitric oxide-modulating amino acids on coronary vessels: relevance to sepsis, Eur. J. Pharmacol. 389 (2000) 209–215.
[12] F.H. Khadour, D. Panas, P. Ferdinandy, C. Schulze, T. Csont, M.M. Lalu, S.M. Wildhirt, R. Schulz, Enhanced NO and superoxide generation in dysfunctional hearts from endotoxemic rats, Am. J. Physiol. Heart Circ. Physiol. 283 (2002) H1108–H1115.
[13] G. Salama, E.V. Menshikova, J.J. Abramson, Molecular interaction between nitric oxide and ryanodine receptors of skeletal and cardiac sarcoplasmic reticulum, Antioxid. Redox Signal. 2 (2000) 5–16.
[14] D. Stoyanovsky, T. Murphy, P.R. Anno, Y.M. Kim, G. Salama, Nitric oxide activates skeletal and cardiac ryanodine receptors, Cell Calcium 21 (1997) 19–29.
[15] X. Zhu, O.Y. Bernecker, N.S. Manohar, R.J. Hajjar, J. Hellman, F. Ichinose, H.H. Valdivia, U. Schmidt, Increased leakage of sarcoplasmic reticulum Ca^{2+} contributes to abnormal myocyte Ca^{2+} handling and shortening in sepsis, Crit. Care Med. 33 (2005) 598–604.

[16] S.M. Harrison, E. McCall, M.R. Boyett, The relationship between contraction and intracellular sodium in rat and guinea-pig ventricular myocytes, J. Physiol. 449 (1992) 517–550.

[17] D.J. Duncan, P.M. Hopkins, S.M. Harrison, Negative inotropic effects of tumour necrosis factor-α and interleukin-1β are ameliorated by alfentanil in rat ventricular myocytes, Br. J. Pharmacol. 150 (2007) 720–726.

[18] A. Kumar, R. Brar, P. Wang, L. Dee, G. Skorupa, F. Khadour, R. Schulz, J.E. Parrillo, Role of nitric oxide and cGMP in human septic serum-induced depression of cardiac myocyte contractility, Am. J. Physiol. 276 (1999) R265–R276.

[19] Z. Yang, S.M. Harrison, D.S. Steele, ATP-dependent effects of halothane on SR Ca^{2+} regulation in permeabilized atrial myocytes, Cardiovasc. Res. 65 (2005) 167–176.

[20] E. Picht, A.V. Zima, L.A. Blatter, D.M. Bers, SparkMaster: automated calcium spark analysis with ImageJ, Am. J. Physiol. Cell Physiol. 293 (2007) C1073–C1081.

[21] X.P. Sun, N. Callamaras, J.S. Marchant, I. Parker, A continuum of InsP3-mediated elementary Ca^{2+} signalling events in *Xenopus* oocytes, J. Physiol. 509 (1998) 67–80.

[22] W.K. Chandler, S. Hollingworth, S.M. Baylor, Simulation of calcium sparks in cut skeletal muscle fibers of the frog, J. Gen. Physiol. 121 (2003) 311–324.

[23] D.A. Eisner, A.W. Trafford, M.E. Diaz, C.L. Overend, S.C. O'Neill, The control of Ca release from the cardiac sarcoplasmic reticulum: regulation versus autoregulation, Cardiovasc. Res. 38 (1998) 589–604.

[24] V. Lukyanenko, S. Viatchenko-Karpinski, A. Smirnov, T.F. Wiesner, S. Gyorke, Dynamic regulation of sarcoplasmic reticulum Ca^{2+} content and release by luminal Ca^{2+}-sensitive leak in rat ventricular myocytes, Biophys. J. 81 (2001) 785–798.

[25] H. Cheng, M.R. Lederer, W.J. Lederer, M.B. Cannell, Calcium sparks and [Ca^{2+}]$_i$ waves in cardiac myocytes, Am. J. Physiol. 270 (1996) C148–C159.

[26] M. Keller, J.P. Kao, M. Egger, E. Niggli, Calcium waves driven by "sensitization" wave-fronts, Cardiovasc. Res. 74 (2007) 39–45.

[27] H. Tanaka, T. Sekine, T. Kawanishi, R. Nakamura, K. Shigenobu, Intrasarcomere [Ca^{2+}] gradients and their spatio-temporal relation to Ca^{2+} sparks in rat cardiomyocytes, J. Physiol. 508 (1998) 145–152.

[28] J.W. Bassani, W. Yuan, D.M. Bers, Fractional SR Ca release is regulated by trigger Ca and SR Ca content in cardiac myocytes, Am. J. Physiol. 268 (1995) C1313–C1319.

[29] S.R. Walsh, T. Tang, C. Wijewardena, S.I. Yarham, J.R. Boyle, M.E. Gaunt, Postoperative arrhythmias in general surgical patients, Ann. R. Coll. Surg. Engl. 89 (2007) 91–95.

[30] K. Schlotthauer, D.M. Bers, Sarcoplasmic reticulum Ca^{2+} release causes myocyte depolarization. Underlying mechanism and threshold for triggered action potentials, Circ. Res. 87 (2000) 774–780.

[31] M. Rubart, D.P. Zipes, Mechanisms of sudden cardiac death, J. Clin. Invest. 115 (2005) 2305–2315.

[32] F.G. Akar, The perfect storm: defective calcium cycling in insulated fibers with reduced repolarization reserve, Circ. Res. 101 (2007) 968–970.